

# Pressurized phase transition cascade in $\text{BaMn}_2\text{P}_2$ and $\text{BaMn}_2\text{As}_2$

N. S. Pavlov\* and I. A. Nekrasov

*Institute for Electrophysics, Russian Academy of Sciences, Ekaterinburg 620016, Russia and  
P.N. Lebedev Physical Institute, Russian Academy of Sciences, Moscow, 119991, Russia*

I. R. Shein

*Institute of Solid State Chemistry, Ekaterinburg, 620108, Russia*

(Dated: June 7, 2024)

The structural analogue of iron-based superconductors the  $\text{BaMn}_2\text{P}_2$  and  $\text{BaMn}_2\text{As}_2$  compounds under hydrostatic pressure upto 140 GPa were studied within the framework of DFT+U. The transition from an antiferromagnetic (AFM) insulator to an antiferromagnetic metal is observed under pressure of 6.4 GPa for  $\text{BaMn}_2\text{P}_2$  and 8.3 GPa for  $\text{BaMn}_2\text{As}_2$ . This second order phase transition to the AFM metallic state provides an appropriate normal state for possible superconductivity in these materials. Moreover, a further increase in pressure leads to a series of first order magnetostructural phase transitions between different antiferromagnetic phases, then to a ferromagnetic metal and finally to a nonmagnetic metal. In case of doping these compounds could potentially be a superconductors under pressure (above 6-8 GPa) with critical temperature growing under pressure.

## I. INTRODUCTION

The interest to the family of iron-based high-temperature superconducting pnictides and chalcogenides (see reviews [1–3]) gave rise to the search for new families of chemical and/or structural analogues of these systems (see, e.g. [4, 5]). One of such family are materials with complete substitution of Fe by other chemical elements, for example, manganese Mn. Since Mn is a magnetic ion due to the half filled 3d shell most of its compounds are magnetic. However, in case external pressure is applied the magnetism could be suppressed. Thus a possibility of superconductivity appears.

First superconductivity observation in Mn-based system was done in 2021 for MnSe compound with  $T_c \sim 9$  K at 35 GPa [6]. For another compound  $\text{BaMn}_2\text{As}_2$ , structural analogue of the  $\text{BaFe}_2\text{As}_2$ , the transition to a metallic state with sharp decrease of resistivity below 17 K at 5.8 GPa [7] was experimentally observed. Magnetic measurements were not carried out in [7]. Therefore, the possibility of superconductivity in  $\text{BaMn}_2\text{As}_2$  has not been studied in the detail up to now. The  $\text{BaMn}_2\text{As}_2$  is well studied material at ambient pressure(see, e.g. [8–11]), but under pressure it has not been investigated. Also, the isostructural and isovalent  $\text{BaMn}_2\text{P}_2$  compound under pressure has not been yet studied theoretically or experimentally.

In this paper, the  $\text{BaMn}_2\text{P}_2$  and  $\text{BaMn}_2\text{As}_2$  compounds under external hydrostatic pressures were studied within the framework of DFT+U. The pressure dependence of thermodynamic, structural and magnetic properties of  $\text{BaMn}_2\text{P}_2$  and  $\text{BaMn}_2\text{As}_2$  were obtained from zero pressure upto 140 GPa. The second order phase transition from an antiferromagnetic (AFM) insulator to an AFM metal state is observed under pressure of

6.4 GPa for  $\text{BaMn}_2\text{P}_2$  and 8.3 GPa for  $\text{BaMn}_2\text{As}_2$ . With further pressure increase a series of first order magnetostructural phase transitions between several antiferromagnetic metallic phases, then into a ferromagnetic metal and finally into a nonmagnetic metal is found. The antiferromagnetic phases could potentially be a superconducting ones under pressure (above 6-8 GPa) with critical temperature increasing with pressure possibly up to the typical value corresponding to iron pnictides.

## II. COMPUTATIONAL DETAILS

The calculations were performed in the DFT+U approximation within the VASP software package [12]. The generalized gradient approximation (GGA) in the form of the Perdew-Burke-Ernzerhof (PBE) exchange-correlation functional [13] was employed. The strong onsite Coulomb repulsion of Mn-3d electrons was described with the DFT+U scheme with the Dudarev approach [14]. The U values were taken:  $U = 1.4$  eV for  $\text{BaMn}_2\text{As}_2$  and  $U = 1.2$  eV for  $\text{BaMn}_2\text{P}_2$ . The applied hydrostatic pressure is simulated by reduction of the unit cell volume. The ion positions and lattice constants for certain volume are obtained during the DFT optimization. The Gibbs2 software package [15] is employed to operate with Birch–Murnaghan equation of state [16].

## III. RESULTS AND DISCUSSION

Here we consider the most typical colinear magnetic structures for  $I4/mmm$  space group of symmetry: the non-magnetic (NM), ferromagnetic (FM) and antiferromagnetic (AFM-A, AFM-C, AFM-G types) phases to understand which one is the ground state at a given pressure  $P$  (e.g. to find a minima of total energy  $E(P)$ ).

From the computational point of view the unit cell volume  $V$  is well defined parameter while corresponding

\* pavlov@iep.uran.ru

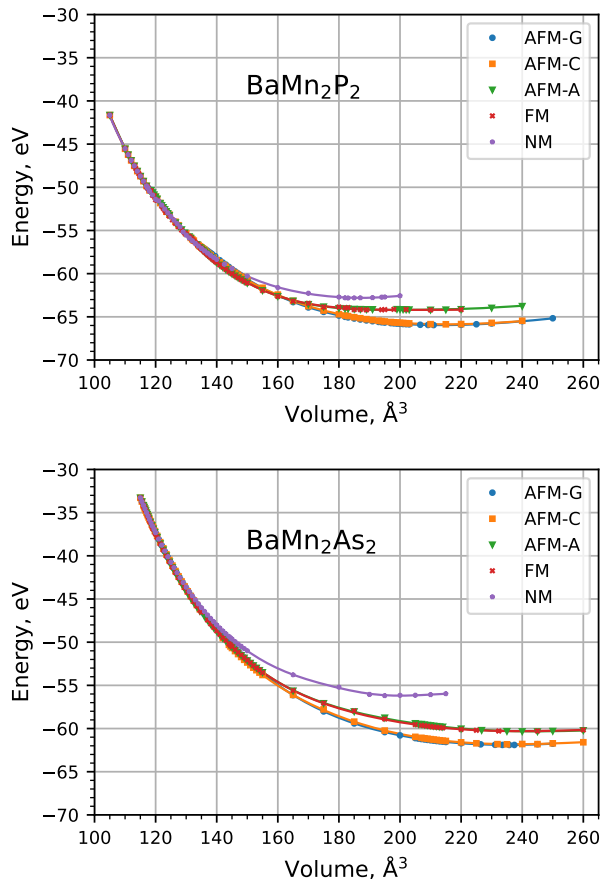


FIG. 1. Total energy  $E$  vs. unit cell volume  $V$  for  $\text{BaMn}_2\text{P}_2$  (top) and  $\text{BaMn}_2\text{As}_2$  (bottom) obtained by GGA+U are plotted with symbols for all considered phases. Solid lines - fit of GGA+U data to Birch-Murnaghan equation of state.

pressure value  $P$  needs to be somehow determined. First that can be done is to calculate total energy as a function of  $V$  around the minima of  $E(V)$  which was estimated by full lattice DFT optimization. Corresponding results are presented in Fig. 1 with symbols for all considered phases (see the legend). Solid lines are a fit of GGA+U data to Birch-Murnaghan equation of state [16]. Once we know the equation of state one can obtain total energy  $E$  as a function of pressure  $P$ .

In Figure 2 the  $E(P)$  related to AFM-G phase (which is found to be a ground state at  $P = 0$  GPa) for all phases is shown. The intervals of different phases stability are separated by vertical lines. Hereafter to plot pressure dependencies of different parameters we will use  $P$  values out of Birch-Murnaghan equation of state.

The first phase transition from AFM-G insulator to AFM-G metal occurs at pressure 6.4 GPa for  $\text{BaMn}_2\text{P}_2$  and at 8.3 GPa for  $\text{BaMn}_2\text{As}_2$ . Corresponding closing of the energy gap can be seen in Figure 3 (bottom panel). Since the gap closes continuously and magnetic order does not change there one can assume second order phase transition (Slater scenario).

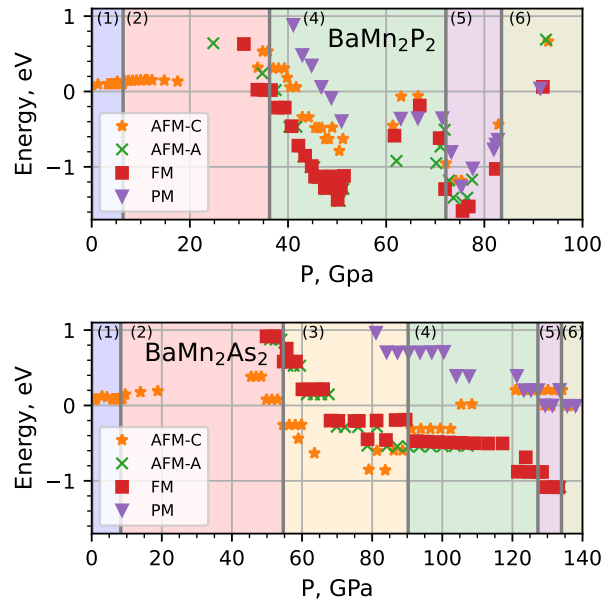


FIG. 2. GGA+U total energies  $E$  for  $\text{BaMn}_2\text{P}_2$  (top) and  $\text{BaMn}_2\text{As}_2$  (bottom) as a function of pressure  $P$  with respect to AFM-G phase. (1) - AFM-G insulator, (2) - AFM-G metal, (3) - AFM-C metal, (4) - AFM-A metal, (5) - FM metal, (6) - non-magnetic metal. The vertical lines correspond to phase transition boundaries.

Then the situation for  $\text{BaMn}_2\text{P}_2$  and  $\text{BaMn}_2\text{As}_2$  becomes different. At 36 GPa the AFM-A metallic solution becomes the ground state for  $\text{BaMn}_2\text{P}_2$ . Then from 72 GPa to 83 GPa  $\text{BaMn}_2\text{P}_2$  is obtained to be a ferromagnetic metal. Above 83 GPa the Mn magnetic moment in FM phase turns to be zero (see Figure 3 top panel on the left side) and  $\text{BaMn}_2\text{P}_2$  goes to a paramagnetic metallic ground state.

For  $\text{BaMn}_2\text{As}_2$  the AFM-G metallic ground state undergoes to AFM-C metallic ground state at 54 GPa. Then the AFM-A phase appears to be the ground state between 90 GPa and 127 GPa. Further antiferromagnetism is suppressed at 127 GPa where a phase transition from metallic AFM-A to metallic FM phase occurs. Then above 134 GPa the Mn magnetic moment in FM phase disappears (see Figure 3 top panel on the right side) and the  $\text{BaMn}_2\text{As}_2$  compound turns to a paramagnetic metal.

Let us note that there are no AFM-G solution for  $\text{BaMn}_2\text{P}_2$  compound above 43 GPa, whereas for  $\text{BaMn}_2\text{As}_2$  compound the AFM-G solution exists up to the transition to the nonmagnetic ground state. Also one can clearly see jumps of the Mn magnetic moment at the phase transitions boundary (see Figure 3 top panels). The values of those jumps are bigger for the phosphorous system than for the arsenic one. The change of magnetic order and presence of those jumps of magnetic moment at phase boundary let us assume first order magnetic phase transitions.

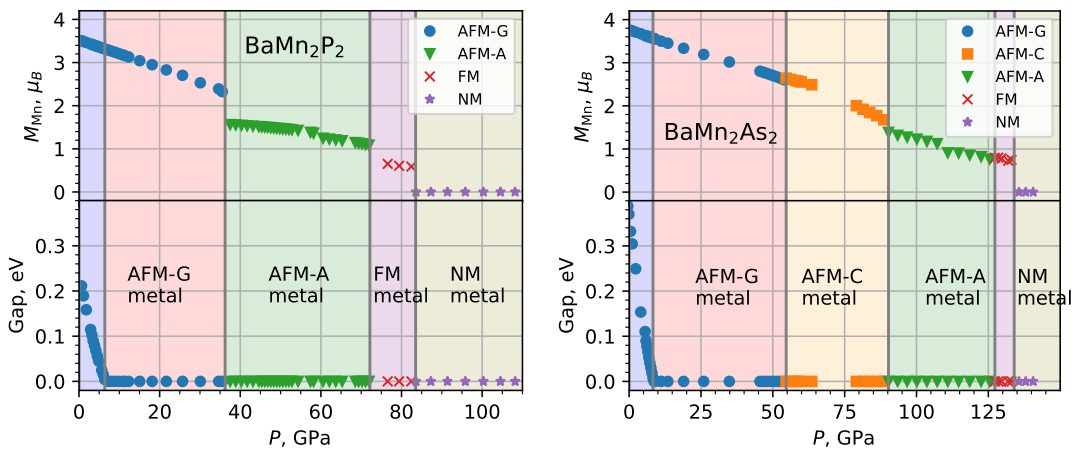


FIG. 3. GGA+U dependence of Mn magnetic moment and energy gap on pressure  $P$  for  $\text{BaMn}_2\text{P}_2$  (left) and  $\text{BaMn}_2\text{As}_2$  (right). Here we present data only for those phases which are ground states.

To more thoroughly investigate the nature of the phase transitions we also analyze structural parameters of the materials under pressure. In Figure 4 the GGA+U dependencies of structural parameters:  $a$ ,  $c$ , As-Fe-As bond angle and anion height with respect to Mn plane  $\Delta z$  on pressure for  $\text{BaMn}_2\text{P}_2$  and  $\text{BaMn}_2\text{As}_2$  are presented. It was found that all observed magnetic phase transitions are accompanied by a jumps of the lattice parameters (see Figure 4). That jumps correspond to a first order magnetostructural phase transitions.

For  $\text{BaMn}_2\text{P}_2$  the value of total density of states at the Fermi level  $N(E_F)$  for prospective from the superconductivity existence point of view metallic AFM-G phase lays in range 0.2–2 states/eV/cell and for metallic AFM-A phase – from 2 to 3 states/eV/cell (Figure 4). As it is well known for iron-based superconductors  $N(E_F)$  has the value from 2 to 5 states/eV/cell for paramagnetic case [17]. In case of  $\text{BaMn}_2\text{As}_2$  the  $N(E_F)$  value for metallic AFM-G phase is almost zero but for metallic AFM-C and AFM-A phases is large enough: 2-3 states/eV/cell. One can clearly see the uptrend of  $N(E_F)$  in pressure for both materials  $\text{BaMn}_2\text{P}_2$  and  $\text{BaMn}_2\text{As}_2$ . Therefore, in principle, one can expect that under pressure (unfortunately, quite large), the superconducting  $T_C$  for AFM manganese pnictides can be of the order of magnitude, but less than for iron-based pnictides.

The pressure dependence  $N(E_F)$  on As-Fe-As bond angle  $\angle\text{As-Fe-As}$  and anion height with respect to Mn plane  $\Delta z$  (Figure 4) is quite different from those for iron-based pnictides without pressure [17]. Under pressure the  $N(E_F)$  has maxima for  $\angle\text{As-Fe-As}$  and  $\Delta z$  far away from ideal ones  $109.5^\circ$  and  $1.37 \text{ \AA}$ , at which the maximum of  $T_c$  is reached for iron pnictides [17].

However overall pressure dependence of  $\angle\text{As-Fe-As}$  and  $\Delta z$  qualitatively agrees rather well for those of iron-based materials under pressure (see *e.g.* [18]). Also for iron pnictides is quite typical a non-monotonic behavior of  $T_c$  with respect to pressure: there is some growth of  $T_c$

upto some certain pressure and then  $T_c$  goes down (see *e.g.* [19]). The same behavior might be expected for manganese materials under consideration because of similar non-monotonic behavior of their  $N(E_F)$  (see Figure 4).

#### IV. CONCLUSION

In this paper, the  $\text{BaMn}_2\text{P}_2$  and  $\text{BaMn}_2\text{As}_2$  compounds under external pressures were studied within the framework of DFT+U. Thermodynamic, structural and magnetic properties of  $\text{BaMn}_2\text{P}_2$  and  $\text{BaMn}_2\text{As}_2$  are presented at pressure from zero to 140 GPa.

The second order phase transition from an AFM-G insulator to a AFM-G metal ground state is observed under pressure of 6.4 GPa for  $\text{BaMn}_2\text{P}_2$  and 8.3 GPa for  $\text{BaMn}_2\text{As}_2$ . Our computational results for  $\text{BaMn}_2\text{As}_2$  suggests that experimentally observed in Ref. [7] metallic state below 17 K at 5.8 GPa could be an antiferromagnetic one.

Then the cascade of first order magnetostructural phase transitions: AFM-G metallic phase, AFM-A metallic phase, FM metallic phase and finally non-magnetic metallic phase for  $\text{BaMn}_2\text{P}_2$  are occurred at 36 GPa, 72 GPa and 83 GPa, correspondingly.

The phase transition cascade for  $\text{BaMn}_2\text{As}_2$  under pressure is slightly different: AFM-G metal, AFM-C metal, AFM-A metal, FM metal and to nonmagnetic metal take place at 54 GPa, 90 GPa, 127 GPa and 134 GPa, respectively.

Also we obtained for manganese materials under consideration non-monotonic pressure behavior of their  $N(E_F)$ : there is some growth of  $T_c$  upto some certain pressure and then  $N(E_F)$  goes down. Once we suppose that  $T_c$  and  $N(E_F)$  are connected in a BCS manner one can expect similar non-monotonic behavior of  $T_c$  with respect to pressure for manganese systems as those experimentally observed for iron pnictides (see *e.g.* [19]). Since

$N(E_F)$  values are nearly the same either for considered manganese materials and typical iron pnictides, in principle, one can expect that under pressure (unfortunately, quite large), the superconducting  $T_c$  for manganese pnictides can be of the order of magnitude, but less (due to its AFM normal state) than for iron-based pnictides.

### ACKNOWLEDGMENTS

The work support of the State Assignments #124022200005-2 of Institute of Electrophysics and

#124020600024-5 of Institute of Solid State Chemistry UB RAS. We are grateful to E.Z. Kuchinskii and P.A. Igoshev for useful discussions.

### APPENDIX

For completeness, the Figure 5 shows pressure dependence of different interatomic distances on pressure for  $\text{BaMn}_2\text{P}_2$  and  $\text{BaMn}_2\text{As}_2$ . Our data qualitatively agrees rather well for those of iron-based materials under pressure (see *e.g.* [18]).

- 
- [1] M. V. Sadovskii, *Physics-Uspekhi* **51**, 1201 (2008), [*Usp. Fiz. Nauk* **2008**, 178, 1243-1271].
  - [2] G. R. Stewart, *Reviews of Modern Physics* **83**, 1589 (2011).
  - [3] K. Ishida, Y. Nakai, and H. Hosono, *Journal of the Physical Society of Japan* **78**, 062001 (2009).
  - [4] M. Neupane, C. Liu, S.-Y. Xu, Y.-J. Wang, N. Ni, J. M. Allred, L. A. Wray, N. Alidoust, H. Lin, R. S. Markiewicz, A. Bansil, R. J. Cava, and M. Z. Hasan, *Physical Review B* **85**, 094510 (2012).
  - [5] I. A. Nekrasov and M. V. Sadovskii, *JETP Letters* **99**, 598 (2014), [*Pis'ma Zh. Eksp. Teor. Fiz.* **2014**, 99, 687].
  - [6] T. L. Hung, C. H. Huang, L. Z. Deng, M. N. Ou, Y. Y. Chen, M. K. Wu, S. Y. Huyan, C. W. Chu, P. J. Chen, and T. K. Lee, *Nature Communications* **12**, 5436 (2021).
  - [7] A. T. Satya, A. Mani, A. Arulraj, N. V. C. Shekar, K. Vinod, C. S. Sundar, and A. Bharathi, *Phys. Rev. B* **84**, 180515 (2011).
  - [8] Y. Singh, A. Ellern, and D. C. Johnston, *Physical Review B* **79**, 2 (2009).
  - [9] A. Pandey, V. K. Anand, and D. C. Johnston, *Physical Review B* **84**, 1 (2011).
  - [10] A. Antal, T. Knoblach, Y. Singh, P. Gegenwart, D. Wu, and M. Dressel, *Physical Review B* **86**, 1 (2012).
  - [11] W. L. Zhang, P. Richard, A. Van Roekeghem, S. M. Nie, N. Xu, P. Zhang, H. Miao, S. F. Wu, J. X. Yin, B. B. Fu, L. Y. Kong, T. Qian, Z. J. Wang, Z. Fang, A. S. Sefat, S. Biermann, and H. Ding, *Physical Review B* **94**, 1 (2016).
  - [12] G. Kresse and J. Furthmüller, *Physical Review B* **54**, 11169 (1996).
  - [13] J. P. Perdew, K. Burke, and M. Ernzerhof, *Physical Review Letters* **77**, 3865 (1996).
  - [14] S. L. Dudarev, G. A. Botton, S. Y. Savrasov, C. J. Humphreys, and A. P. Sutton, *Physical Review B* **57**, 1505 (1998).
  - [15] A. Otero-de-la Roza and V. Luaña, *Computer Physics Communications* **182**, 1708 (2011).
  - [16] F. Birch, *Phys. Rev.* **71**, 809 (1947).
  - [17] E. Z. Kuchinskii, I. A. Nekrasov, and M. V. Sadovskii, *JETP Letters* **91**, 518 (2010).
  - [18] K. Kobayashi, J.-i. Yamaura, S. Iimura, S. Maki, H. Sagayama, R. Kumai, Y. Murakami, H. Takahashi, S. Matsuishi, and H. Hosono, *Scientific Reports* **6**, 39646 (2016).
  - [19] A. S. Sefat, *Reports on Progress in Physics* **74**, 124502 (2011).

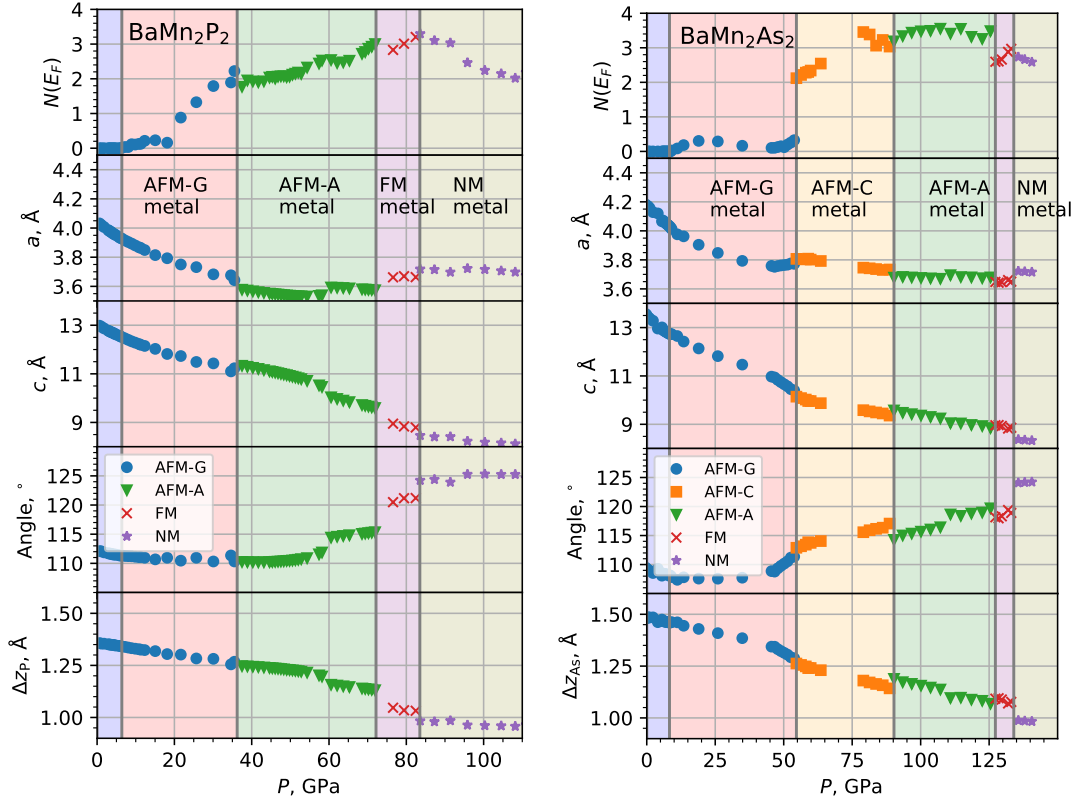


FIG. 4. GGA+U dependence of total density of states at the Fermi level  $N(E_F)$ , lattice constants  $a$  and  $c$ , As-Fe-As bond angle and anion height with respect to Mn plane  $\Delta z$  on pressure for BaMn<sub>2</sub>P<sub>2</sub> (left) and BaMn<sub>2</sub>As<sub>2</sub> (right). Here we present data only for those phases which are the ground states.

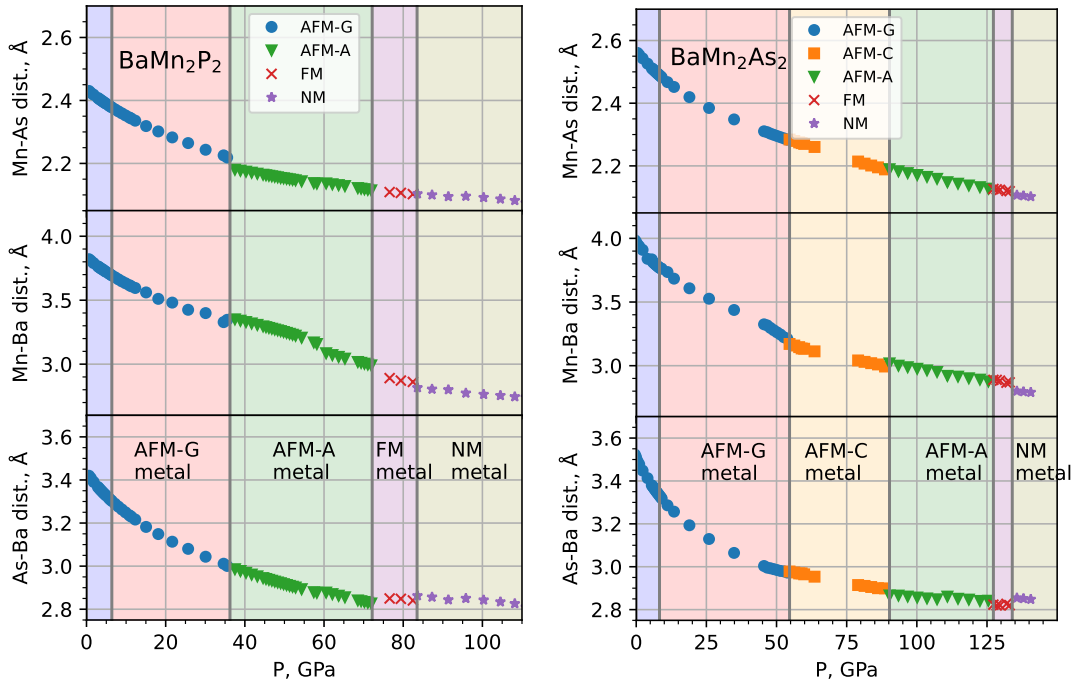


FIG. 5. GGA+U dependence of different interatomic distances on pressure for BaMn<sub>2</sub>P<sub>2</sub> (left) and BaMn<sub>2</sub>As<sub>2</sub> (right). Here we present data only for those phases which are ground states.